### Stoneley-wave attenuation and dispersion in permeable formations

Andrew N. Norris\*

#### ABSTRACT

The tube wave, or low-frequency manifestation of the Stoneley wave, has been modeled previously using the quasi-static approximation; I extend this method to include the effect of the formation matrix compressibility, which tends to marginally increase the tube-wave attenuation. Using the Biot theory of poroelasticity, I develop a fully dynamic description of the Stoneley wave. The dispersion relation derived from Biot's equations reduces in the low-frequency limit to the quasi-static dispersion relation. Comparisons of the quasi-static and dynamic theories for typical sandstones indicate the former to be a good approximation to at least 1 kHz for oil and water infiltration. At higher frequencies, usually between 5 and 20 kHz for the formations considered, a maximum in the Stoneley Q is predicted by the dynamic theory. This phenomenon cannot be explained by the quasi-static approximation, which predicts a constantly increasing Q with frequency. Instead, the peak in Q may be understood as a transition from dispersion dominated by bore curvature to a higher frequency regime in which the Stoneley wave behaves like a wave on a flat fluid-porous interface. This hypothesis is supported by analytical and numerical results.

#### INTRODUCTION

The attenuation of the Stoneley wave in the presence of formation pore-fluid mobility is well known and has been proposed as a means of measuring permeability (Alhilali and Zemanek, 1984). Quantitative modeling by Rosenbaum (1974), Schmitt and Bouchon (1984), and by Schmitt et al. (1988) supports the conclusion that attenuation increases with permeability and with pore fluid mobility; i.e., attenuation decreases as pore-fluid viscosity increases. Rosenbaum based his findings on synthetic acoustic signals covering a wide range of frequencies. Schmitt et al. (1988) examined the effects of individual factors, such as interface permeability, pore fluid, and bore radius, and also discussed the first pseudo-Rayleigh wave

mode. Others, particularly White (1983) and Mathieu and Toksöz (1984), considered the low-frequency quasi-static regime in which the Stoneley wave is often referred to as the tube wave. They obtained explicit analytical results that indicate attenuation increases with porosity, permeability, and frequency, but decreases with bore radius. Hsui and Toksöz (1986) drew similar conclusions from an approximate dynamic model for the Stoneley wave; however, as discussed below, some of their numerical calculations appear to be in error. The general findings of these various theoretical calculations are in agreement with measured data (Williams et al., 1984; Burns and Cheng, 1986). Liu (1988) recently considered the influence of permeability on the modes of a cylindrical sample submerged in fluid.

The present study examines Stoneley-wave attenuation over the full frequency range of acoustic logging. The objective is not to reproduce the findings of the references mentioned, but to understand the underlying mechanisms. In the quasi-static regime, the tube-wave dissipation is well known (White, 1983) to result from diffusion of pore pressure into the surrounding formation via the connected pore network. This dissipative mechanism is still effective at higher frequencies, as suggested by Rosenbaum's (1974) calculations. However, it is complicated by the coupling between pore pressure diffusion and purely geometrical dispersive effects found in elastic formations. The latter subject is well treated in the literature of full-wave acoustic logging, beginning with Biot (1952). Recent references are listed by Schmitt and Bouchon (1985), while Stevens and Day (1986) focus on the low-frequency dispersion.

The first half of this paper considers in detail the quasistatic theory of tube-wave dispersion and attenuation. This theory, which by definition ignores all inertial effects except that of the bore fluid, was developed by White (1983). The main result of this part of the paper is an extension of White's analysis to include the compressibility of the matrix grain. This is necessary to verify the fully dynamic theory for a compressible matrix, which is considered later. It is shown that frame compressibility decreases the pore-pressure diffusion coefficient but increases the tube-wave attenuation. The results of the quasi-static theory are compared with those for a rigid frame (White, 1983) and also with the theory of Mathieu and Toksöz (1984).

Manuscript received by the Editor June 26, 1986; revised manuscript received September 1, 1988.

1989 Society of Exploration Geophysicists. All rights reserved.

<sup>\*</sup>Department of Mechanics and Materials Science, Rutgers University, P.O. Box 909, Piscataway, NJ 08855-0909.

The remainder of the paper considers the dispersion and attenuation of the Stoneley wave at higher frequencies. Biot's theory of dynamic poroelasticity is used to derive the dispersion equation. It is shown how the previously determined quasi-static tube-wave speed in a compressible frame drops out of the fully dynamic theory in the appropriate limit. Numerical results for fluid-saturated sandstones indicate the range of validity of the quasi-static theory and also a possible peak in the Stoneley Q. This phenomenon is explained in terms of a Stoneley wave on a flat fluid-porous interface.

## PORE-PRESSURE DIFFUSION IN A COMPRESSIBLE FRAME

Before considering tube-wave attenuation in a permeable formation, it is necessary to define precisely the diffusion coefficient to be used. This is done for two reasons: first, previous treatments (White, 1983; Mathieu and Toksöz, 1984) have not considered the effects of frame compressibility; second, the quasi-static limit of the dynamic dispersion relation derived below in equation (24) explicitly contains frame compressibility, so any quasi-static theory that ignored frame compressibility would not be in agreement. The quasi-static analysis is thus necessary as a check on the fully dynamic results discussed later. It is also useful in its own right, but its range of validity is uncertain at this stage.

Quasi-static fluid flow through a permeable solid is governed by Darcy's law

$$\frac{\partial \mathbf{w}}{\partial t} = -\frac{\kappa}{\eta} \, \nabla p,\tag{1}$$

where  $\kappa$  is the permeability,  $\eta$  the viscosity,  $\mathbf{w}$  the incremental fluid displacement relative to the matrix, and p the incremental pore pressure. In a rigid or incompressible matrix, the volumetric strain in the pore fluid satisfies Hooke's law for an inviscid fluid

$$-\nabla \cdot \mathbf{w} = \frac{\Phi}{K_f} p, \tag{2}$$

where  $\phi$  is the porosity and  $K_f$  is the pore-fluid bulk modulus. Eliminating w from equations (1) and (2) gives the pressure diffusion equation

$$C_0 \nabla^2 p = \frac{\partial p}{\partial t},\tag{3}$$

with the diffusion coefficient

$$C_0 = \frac{\kappa}{\eta} \frac{K_f}{\phi}.$$
 (4)

A simple (e.g., Marsily, 1981) but inexact way to compensate for the matrix compressibility is to augment the strain  $-\nabla \cdot \mathbf{w}$  in equation (2) with the quantity p/K, where K is the bulk modulus of the frame under drained conditions (see Appendix A). The diffusion coefficient is then

$$C_1 = C_0 / \left( 1 + \frac{K_f}{\phi K} \right). \tag{5}$$

A more precise analysis for diffusion in an elastic matrix follows by using Biot's poroelastic stress-strain relations (A-1) and (A-2) instead of equation (2). Briefly, equation (A-2) and

the trace of equation (A-1) imply that  $\nabla \cdot \mathbf{w} = (-K_c/KM)p'$ , where  $p' = p + (\alpha M/3K_c)\tau_{kk}$ . (See Appendix A for the definitions of  $\tau_{ij}$ ,  $\alpha$ , M, K, and  $K_c$ .) Also, the static equilibrium equations  $\tau_{ij,\ j} = 0$  imply  $\tau_{ij,\ ij} = 0$ , which, with equations (A-1) and (A-2), gives  $K(K_c + \frac{4}{3}\mu)\nabla^2 p = K_c(K + \frac{4}{3}\mu)\nabla^2 p'$ . In all cases of practical concern, the pressure p goes to zero uniformly at infinity. The condition for the borehole geometry of interest here is that  $p \to 0$  as  $r \to \infty$ . Direct integration then yields  $K(K_c + \frac{4}{3}\mu)p = K_c(K + \frac{4}{3}\mu)p'$ . Now we take the divergence of Darcy's law, equation (1), and eliminate  $\nabla \cdot \mathbf{w}$  to get

$$C \nabla^2 p = \frac{\partial p}{\partial t},\tag{6}$$

where the modified diffusion coefficient is

$$C = C_0 / \left\{ 1 + \frac{K_f}{\phi K} \left[ (1 - \alpha)(\alpha - \phi) + \alpha^2 \left( 1 + \frac{4\mu}{3K} \right)^{-1} \right] \right\}.$$
 (7)

The diffusion coefficient C has been derived and discussed by Jaeger and Cook (1969), Rice and Cleary (1976), and Chandler and Johnson (1981) among others, but it appears that no quantitative comparison of C,  $C_0$ , and  $C_1$  has been given. It is shown in Appendix B that  $\alpha > \phi$ . It then follows from equations (5) and (7) that

$$C_1 < C < C_0$$
. (8)

The simple coefficient  $C_1$  therefore overestimates the decrease in diffusivity due to the matrix compressibility. However, a better lower bound for C exists in the form  $C_2 < C$ , where  $C_2 = C_0/(1 + K_f/\Phi K_s) > C_1$ , and  $K_s$  is the bulk modulus of the grain (see Appendix A).

The distinction between the Biot diffusion coefficient C and the simpler  $C_0$  is obviously negligible when the pore fluid is much more compressible than the matrix, as for example, in gas-saturated sandstone. Table 3 lists the values of  $C/C_0$  for the sandstones and pore fluids in Tables 1 and 2. The ratio is very nearly unity for gaseous infiltration, but can be appreciably less for water saturation. Frame compressibility is very significant for loosely consolidated materials such as soil, for which the frame modulus satisfies  $K \ll K_s$ ,  $K_f$ . For this case, it follows from equations (A-3)–(A-5) and (7) that  $1/K_c \approx \Phi/K_f + (1-\Phi)/K_s$  (Wood's formula),  $M \approx K_c$ , and  $C/C_0 \approx \Phi(K+\frac{4}{3}\mu)/K_f \ll 1$ . Other limiting forms of C are discussed by Chandler and Johnson (1981).

## LOW-FREQUENCY TUBE-WAVE ATTENUATION AND DISPERSION

The tube wave is the commonly used term for the low-frequency Stoneley wave in a borehole. Its speed in an elastic formation is

$$v_T = v_B/(1 + K_B/\mu)^{1/2},$$
 (9)

where  $\mu$  is the formation shear modulus, and  $v_B$  and  $K_B$  are the sound speed and bulk modulus in the bore fluid, related by  $v_B = (K_B/\rho_B)^{1/2}$ , where  $\rho_B$  is the density. The presence of formation permeability provides a dissipative mechanism for the tube wave. The low-frequency speed in a permeable formation can then be defined as the complex quantity  $v = (K^*/\rho_B)^{1/2}$ . The complex effective modulus  $K^*$  is the ratio of the effective

Norris Norris

bore-fluid dilatation to the borehole pressure  $p^B$ . The effective dilatation is the sum of the actual dilatation of the fluid plus the dilatation induced by the formation compressibility and permeability. Thus,

$$\frac{1}{K^*} = \frac{1}{K_B} + \frac{2\pi a}{\pi a^2} \frac{u_r(a) + w_r(a)}{p^B},\tag{10}$$

where  $u_r(a)$  is the quasi-static radial displacement of the borehole of radius a, and  $w_r(a)$  is the radial displacement of the pore fluid relative to the matrix. The static elastic expansion of the bore under the applied pressure  $p^B$  can be solved easily to give  $u_r(a) = p^B a/2\mu$  (White, 1983). In the absence of permeability,  $w_r(a) = 0$  and  $v = v_T$  [equation (9)].

The ratio  $w_r(a)/p^B$  in equation (10) can be obtained for a permeable formation by solving equation (6) for p(r, t) in r > a subject to time harmonic pressure at the interface  $p(a, t) = p^B e^{-i\omega t}$ . The solution can be found in terms of Bessel functions, and  $w_r(a)$  then follows from equation (1) as

$$\frac{w_r(a)}{p^B} = \frac{\kappa}{\eta} \frac{a}{2C} E\left(a^2 \frac{\omega}{C}\right),\tag{11}$$

where

$$E(x) = \frac{-2}{\sqrt{ix}} \frac{H_1^{(1)}(\sqrt{ix})}{H_0^{(1)}(\sqrt{ix})},$$
 (12)

and  $H_0^{(1)}$  and  $H_1^{(1)}$  are Hankel functions of the first kind. The tube-wave speed follows from equation (10) and  $v = (K^*/\rho_B)^{1/2}$  as

$$\frac{1}{v^2} = \frac{1}{v_T^2} + \frac{\phi}{v_f^2} \frac{\rho_B}{\rho_f} \frac{C_0}{C} E\left(a^2 \frac{\omega}{C}\right). \tag{13}$$

The complex function E(x) is plotted in Figure 1. Note that  $E(x) \rightarrow 2(i/x)^{1/2}$  as  $x \rightarrow \infty$ .

Values of  $a^2\omega/C$ , the argument of E in equation (13) and given in Table 3 for the combinations of sandstones and pore fluids in Tables 1 and 2, are all greater than 3 at 1 kHz frequency. Assuming that  $a^2\omega/C\gg 1$ , the open pore tube-wave speed of equation (13) can be approximated as

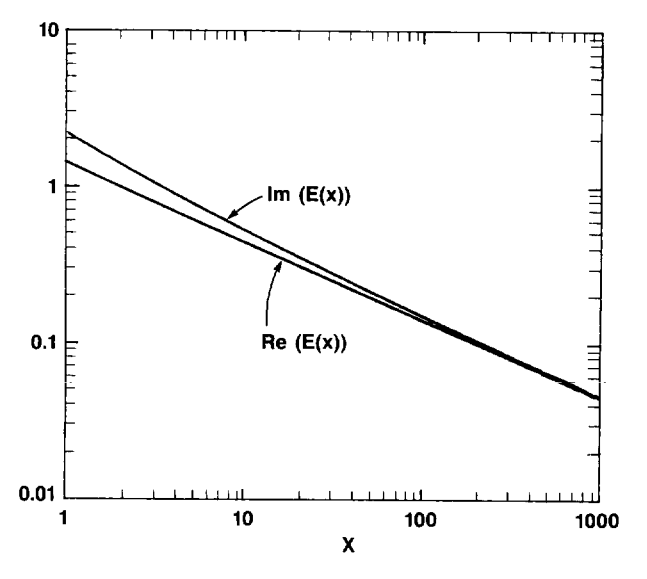


Fig. 1. The function E(x) of equation (12).

Table 1. Dry sandstone data (from Rosenbaum, 1974). The speeds are in meters per second and the permeability in millidarcies (1 Darcy =  $10^{-8}$  cm<sup>2</sup>).

| Sandstone | φ     | v <sub>C, dry</sub><br>(m/s) | $rac{v_{S,\; m dry}}{({ m m/s})}$ | κ<br>(mD) |  |
|-----------|-------|------------------------------|------------------------------------|-----------|--|
| Fox Hill  | 0.074 | 4450                         | 2515                               | 32        |  |
| Berea     | 0.19  | 3670                         | 2170                               | 200       |  |
| Teapot    | 0.30  | 3048                         | 1865                               | 1900      |  |

Table 2. Pore-fluid parameters. Viscosity is in units of grams per centimeter-second and sound speed is in meters per second.

| Fluid        | η<br>(g/cm s)                  | $\rho_f$    | $v_f$ (m/s) |
|--------------|--------------------------------|-------------|-------------|
| Oil          | 1.8                            | 0.88        | 1455        |
| Water<br>Gas | $10^{-2}$ $2.2 \times 10^{-4}$ | 1.0<br>0.14 | 1500<br>630 |

$$v = v_T \left[ 1 - \phi \gamma \frac{K_B}{K_L} \left( \frac{C_0}{C} \right)^{1/2} \left( \frac{iC_0}{a^2 \omega} \right)^{1/2} \right],$$
 (14)

where  $0 < \gamma < 1$  and

$$\gamma = \frac{\mu}{\mu + K_R}.\tag{15}$$

If the dependence of  $(C_0/C)$  upon porosity is ignored, the imaginary part of v in equation (14) scales as  $(\phi \kappa/a^2)^{1/2}$ . This implies that attenuation, which depends upon the imaginary part of v, increases with porosity and permeability and decreases with increasing bore radius (Hsui and Toksöz, 1986).

# Effects of interfacial permeability and intrinsic body-wave attenuation

It has been proposed in the past to modify the pressure continuity condition at the interface by introducing a permeability parameter  $\beta$  such that (Deresiewicz and Skalak, 1963)

$$p^B = p + \beta \frac{\partial w_r}{\partial t}, \quad \text{at} \quad r = a.$$
 (16)

Little is known about the value of  $\beta$  in general, except that it is identically zero when natural boundary conditions for Biot's equations are deduced from variational principles. [See Berryman and Thigpen (1985) for a discussion.] Using equation (16) and proceeding as before, the tube-wave speed is

$$\frac{1}{v^2} = \frac{1}{v_T^2} + \frac{\phi}{v_f^2} \frac{\rho_B}{\rho_f} \frac{C_0}{C} E\left(a^2 \frac{\omega}{C}\right) / \left[1 - \frac{\beta}{2} \frac{i\omega\phi a}{K_f} \frac{C_0}{C} E\left(a^2 \frac{\omega}{C}\right)\right]. \tag{17}$$

The open-pore speed of equation (14) corresponds to  $\beta=0$ . In the closed pore limit;  $\beta=\infty$ , the speed is simply  $v=v_T$ , and there are no pore-fluid effects in the quasi-static theory. This concurs with the conclusions of Rosenbaum (1974), who considered a higher frequency range, and also with those of Schmitt et al. (1988). For this reason the rest of the paper concentrates on the open pore condition.

Let  $Q_{\alpha}$ ,  $\alpha = S$ , C, and B, be the quality factors (White, 1983) for the formation shear waves, formation compressional waves, and borehole acoustic waves. Under the generally valid assumption  $1/Q_{\alpha} \ll 1$ ,  $\alpha = S$ , C, and B, a tube-wave quality factor  $Q_T$  can be defined by  $v^{-1} = v_T^{-1}(1 + i/2Q_T)$ . It follows by perturbation of equation (14) as

$$\frac{1}{Q_T} = \frac{\gamma}{Q_B} + \frac{1 - \gamma}{Q_S} + \frac{\gamma}{Q_P},\tag{18}$$

that  $Q_P$ , a frequency-dependent quality factor attributable to permeability, is

$$Q_{P} = \frac{1}{\Phi} \left( \frac{K_{f}}{K_{R}} \right) \left( \frac{C}{C_{0}} \right)^{1/2} \left( \frac{a^{2} \omega}{2C_{0}} \right)^{1/2}. \tag{19}$$

Values of  $Q_p$  at 1 kHz frequency are given in Table 3 for saturated sandstones. Note the broad range in  $Q_p$ . For a given formation, the importance of pore-flow attenuation can be estimated by comparing the  $Q_p$  term in equation (18) with the other two Q terms.

#### Comparisons with other approximate theories

White's theory for a rigid matrix.—The quasi-static tubewave speed in a permeable formation of equation (13) is similar to that of White (1983) for a rigid frame. His equation has  $C = C_0$ , the diffusion constant for the rigid frame. As equation (8) indicates, the ratio  $C/C_0$  is less than unity. Replacing C with  $C_0$  in equation (13) has the effect of decreasing both the real and imaginary parts of the second term on the right-hand side. Consequently, frame compressibility causes an increase in the tube-wave attenuation in a permeable formation. This result is not obvious: since the diffusion coefficient C is less than its rigid counterpart  $C_0$ , a straightforward substitution in White's theory incorrectly predicts a decrease in attenuation.

**Mathieu's theory.**—Mathieu (1984) and Mathieu and Toksöz (1984) presented an approximate theory for the tubewave attenuation coefficient, defined as  $\alpha = \text{Im } (\omega/v)$ . Let  $\alpha_M$  denote Mathieu's  $\alpha$ , which is

$$\alpha_M = \frac{\rho_B v_T}{a} \frac{\Phi}{Z_n} \left[ k_r a \frac{I_0(k_r a)}{I_1(k_r a)} \right]. \tag{20}$$

Here  $k_r = \omega (v_T^{-2} - v_B^{-2})^{1/2}$  is the radial wavenumber;  $I_0$  and  $I_1$  are modified Bessel functions; and  $Z_P$  is an impedance (Mathieu, 1984) given by

$$\frac{\Phi}{Z_p} = \frac{\kappa}{2\eta a} \left[ 1 + \frac{4}{\pi} \left( \frac{a^2 \omega}{C_0} \right)^{1/2} \right]. \tag{21}$$

The derivation by Mathieu (1984) is implicitly a quasi-static analysis. To be fully consistent, he should have taken the low-frequency approximation  $k_r a \ll 1$  for the bracketed term in equation (20), which becomes 2. This is done in the comparisons below, where it is shown that  $\alpha_m$  is always too large. As the bracketed term is actually greater than 2, its inclusion only worsens matters.

Let  $\alpha = \alpha_T$  be the attenuation derived from equation (13). As mentioned above, the quantity  $x = a^2 \omega/C$  generally satisfies  $x \gg 1$ , particularly above 1 kHz. Therefore, equation (14) can be used for  $\alpha_T$ , and equation (21) also simplifies to give

$$\frac{\alpha_M}{\alpha_T} \approx \frac{4\sqrt{2}}{\pi} \sqrt{\frac{C}{C_0}}.$$

Thus, at higher frequencies for which  $x \gg 1$ , Mathieu's attenuation is correct except for a factor of 1.8  $(C/C_0)^{1/2}$ . At low frequencies, or  $x \ll 1$ , Mathieu's attenuation  $a_M$  tends to the constant  $\rho_B v_T \kappa/2\eta a^2$ . In this frequency range, the approximation of equation (14) is not valid. Instead, equation (13) implies that  $a_T$  is of the order  $[x/|\log(x)|]^{1/2}$ , which tends to zero as  $\omega \to 0$ .

Numerical comparison.—Figure 2 shows the attenuation of the present theory compared with those of White's theory for the rigid matrix and of Mathieu's theory. The curves are for drilling mud,  $\rho_B = 1.4 \text{ g/cm}^3$ ,  $v_B = 1250 \text{ m/s}$ , a bore of radius 10 cm, in a water-saturated Teapot sandstone formation (see Tables 1 and 2). Mathieu theory predicts too large a value, particularly at low frequencies where the present theory is valid. As surmised previously, the attenuation for the rigid matrix is uniformly less than that of the compressible matrix. However, even for this formation, which has the greatest difference between C and  $C_0$  (see Table 3), the effect of matrix compressibility on tube-wave attenuation is small.

Table 3. Some parameters of the porous media formed from the sandstone frames saturated with different fluids. The Biot critical frequency  $f_c = \phi \eta/2\pi\kappa\rho_f T$  follows from equation (A-14), with T=3 for all cases considered.  $Q_P$ , C,  $C_0$ , and  $B_0$  are defined in equations (19), (7), (4), and (A-15), respectively.  $Q_P$  and  $a^2\omega/C$  are both calculated for a frequency of 1 kHz and a=10 cm.

| Pore<br>fluid | Sandstone         | f <sub>c</sub> (kHz)              | $Q_P$ (1 kHz) | $\frac{a^2\omega}{C} (1 \text{ kHz})$ | $\frac{C}{C_0}$ | $B_{0}$     |
|---------------|-------------------|-----------------------------------|---------------|---------------------------------------|-----------------|-------------|
| Oil           | Fox Hill<br>Berea | $2.5 \times 10^4$ $1 \times 10^4$ | 900<br>217    | $1.6 \times 10^4$ $6.8 \times 10^3$   | 0.86<br>0.82    | -8.5 $-6.1$ |
|               | Teapot            | $1.7\times10^3$                   | 55            | $1.2 \times 10^3$                     | 0.77            | -4.6        |
| Water         | Fox Hill          | 123                               | 72.           | 77                                    | 0.84            | -7.2        |
|               | Berea             | 50                                | 17.5          | 33                                    | 0.79            | -5.2        |
|               | Teapot            | 8                                 | 4.4           | 5.9                                   | 0.74            | -4.0        |
| Gas           | Fox Hill          | 19                                | 1.8           | 58                                    | 0.99            | -246        |
|               | Berea             | 8.0                               | 0.46          | 24                                    | 0.99            | -168        |
|               | Teapot            | 1.3                               | 0.12          | 4                                     | 0.99            | -121        |

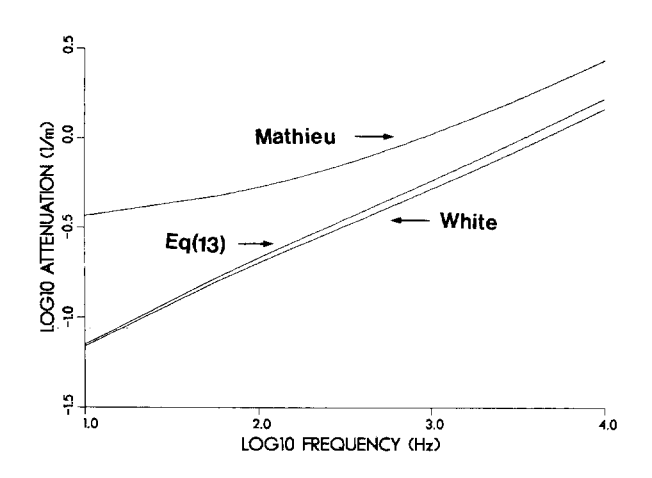


FIG. 2. Plots of attenuation for a Teapot-water permeable formation from 10 to 10 000 Hz comparing the exact low-frequency theory of equation (13), White's model for a rigid matrix, which follows from equation (13) with  $C = C_0$ , and Mathieu's theory of equation (20).

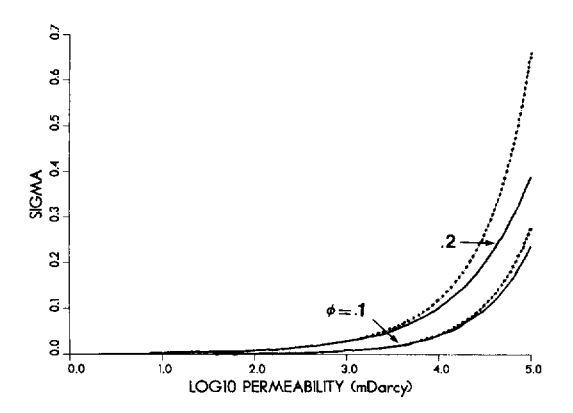


Fig. 3. The dimensionless attenuation  $\sigma = \text{Im} (v_T/v)$  from equations (13) and (22) for  $v_T = 1600$  m/s, a = 10 cm, f = 5 kHz, and  $K_f/\eta = 2 \times 10^{12}$  Hz: The solid line is from equation (13) with  $\rho_B = \rho_f$  and  $v_B = v_f = v_T$ ; the dotted line is from equation (22).

## DYNAMIC THEORY OF STONELEY-WAVE ATTENUATION AND DISPERSION

The complex tube-wave speed v of equation (13) is based upon a quasi-static theory for which  $v_T$  is the appropriate speed in a nonporous formation. No inertial effects were included in the derivation. In order to examine the effect of permeability on the Stoneley wave at higher frequencies, a dynamic theory must be considered that incorporates porefluid flow.

#### The theory of Hsui and Toksöz

Hsui and Toksöz (1986) proposed modeling the Stoneley wave as the fundamental mode in a rigid acoustic waveguide. The coupling to the permeable medium occurs through the pressure and velocity conditions at r = a. Their equation for the complex Stoneley wave speed v is

$$\frac{2}{\lambda} \left(1 - v_T^2/v^2\right)^{1/2} \frac{J_1[\lambda(1 - v_T^2/v^2)^{1/2}]}{J_0[\lambda(1 - v_T^2/v^2)^{1/2}]} + \Phi E\left(\frac{a^2\omega}{C_0}\right) = 0, \quad (22)$$

where  $\lambda = \omega a/v_T$ . Note that as  $\lambda \to 0$ , this equation reduces to the quasi-static equation (13) with  $\rho_B = \rho_f$  and  $v_B = v_f = v_T$ . The dimensionless attenuation  $\sigma = \operatorname{Im} (v_T/v)$  calculated by solving equation (22) is shown in Figure 3, compared with the quasi-static  $\sigma$ . The agreement at low permeability but finite  $\lambda$  is explained as follows: In the limit of small attenuation, the second term in equation (22) is small. Hence the argument of  $J_1$  must also be small and independent of  $\lambda$ , so equation (22) also reduces to the quasi-static theory when the permeability-induced attenuation is small. This equivalence is to be expected, since the fundamental mode of equation (22) with  $\phi = 0$  is the nondispersive solution  $v = v_T$ .

The parameters of Figure 3 are the same as those for Figure 1 of Hsui and Toksöz (1986). However, their curves show uniformly higher values of  $\sigma$  than those in Figure 3. That their results are in error can be confirmed by considering a low value of permeability and solving equation (22) by perturbative methods.

#### Dynamic poroelasticity and Stoneley waves

A better procedure than that of Hsui and Toksöz is to take Biot's (1952) theory for a fluid-filled bore in an elastic formation and augment the equations with Darcy's flow equation (1) with the pore-fluid constitutive equation (2). However, to be fully consistent with the compressible matrix diffusion equations (6) and (7), the formation should be modeled using Biot's (1956, 1962) dynamic theory of poroelasticity (see Appendix A). Biot's theory consistently couples pore-fluid flow with the dynamics of an elastic matrix, and has been derived by many authors using different approaches (e.g., Burridge and Keller, 1981). Biot's theory will be used here to obtain the dispersive behavior of the Stoneley wave.

The dispersion equation is derived in Appendix A for axially symmetric borehole guided modes in a poroelastic formation as

$$D(\omega, h) = \det (\mathbf{M})$$

$$= 0, \tag{23}$$

where  $\mathbf{M}$  is the 4  $\times$  4 complex-valued matrix

$$\begin{bmatrix} \frac{-\xi_{B}}{k_{B}^{2}} \frac{\mu}{K_{B}} f_{2}(\xi_{B}a) & (1+B_{S})k & (1+B_{C})\xi_{C} & (1+B_{D})\xi_{D} \\ 1 & 2k\xi_{S} f_{1}(\xi_{S}a) + 2i \frac{k}{a} \left[ k_{S}^{2} - 2k^{2} + \left(\frac{B_{C} - B_{S}}{B_{S} + \rho/\rho_{f}}\right) k_{S}^{2} \right] f_{1}(\xi_{C}a) + 2i \frac{\xi_{C}}{a} \left[ \frac{\alpha M}{\mu} (B_{D} - B_{O}) k_{D}^{2} - 2k^{2} \right] f_{1}(\xi_{D}a) + 2i \frac{\xi_{D}}{a} \\ 0 & 2k^{2} - k_{S}^{2} & 2k\xi_{C} & 2k\xi_{D} \\ 1 & 0 & (\alpha + B_{C}) \frac{M}{\mu} k_{C}^{2} f_{1}(\xi_{C}a) & (\alpha + B)_{D} \frac{M}{\mu} k_{D}^{2} f_{1}(\xi_{D}a) \end{bmatrix}$$

$$(24)$$

where

and

$$f_1(x) = \frac{-iH_0^{(1)}(x)}{H_1^{(1)}(x)}$$

$$f_2(x) = \frac{-iJ_1(x)}{J_2(x)}.$$
(25)

The various parameters in equation (24) are defined in Appendix A.

#### Low-frequency limit: Comparison with the quasi-static theory

The limit of most relevance to the results of the previous sections, particularly equation (13), is the low-frequency limit  $\omega \ll \omega_c$ , where  $\omega_c$  is defined in equation (A-14). The critical frequency  $f_c = \omega_c/2\pi$  is given in Table 3 for different saturated sandstones. In the low-frequency regime, the quantities ka,  $k_C a$ ,  $k_S a$ , and  $k_B a$  are all much less than 1, while  $|k_D a|$  is of order unity. Also, as discussed in Appendix A,  $B_C$ ,  $B_S \sim 0$ , but  $B_D \sim B_0$ , a negative constant given in Table 3. The wavenumber  $\xi_D \sim k_D \sim (i\omega/C)^{1/2}$ , where C is the diffusion coefficient of equation (7); and  $\mathbf{M} \sim \mathbf{M}_0$ , where

$$M_{\circ} =$$

$$\begin{bmatrix} i\xi_{B}^{2}a\mu & k & \xi_{C} & (1+B_{0})k_{D} \\ 1 & 2i\frac{k}{a} & 2i\frac{\xi_{C}}{a} & 2i\frac{k_{D}}{a} \\ 0 & 2k^{2}-k_{S}^{2} & 2k\xi_{C} & 2kk_{D} \\ 1 & 0 & 0 & (\alpha+B_{0})\frac{M}{\mu}k_{D}^{2}f_{1}(k_{D}a) \end{bmatrix}$$
(26)

Explicit calculation gives, using various relations among the Biot constants (see Appendix A) and defining the phase velocity  $v = \omega/k$ ,

$$\det (\mathbf{M}_0) =$$

$$-2ik_S^2 \xi_C k_D \frac{B_0}{a} \left[ 1 + \left( \frac{1}{v_T^2} - \frac{1}{v^2} \right) \frac{v_f^2}{\phi} \frac{\rho_f}{\rho_B} \frac{C}{C_0} \frac{1}{E(a^2 \omega/C)} \right], \quad (27)$$

where the function E(x) is defined in equation (12). The low-frequency limit of the dispersion equation (23) thus reduces exactly to the quasi-static equation (13).

#### NUMERICAL RESULTS AND DISCUSSION

The same combinations of sandstones (Table 1) and saturants (Table 2) as considered by Rosenbaum (1974) are used here. The elastic moduli K and  $\mu$  of Appendix A are  $\mu = (1 - \phi)\rho_s v_{S,dry}^2$ , and  $K + 4\mu/3 = (1 - \phi)\rho_s v_{C,dry}^2$ , where  $\rho_s = 2.65$  g/cm<sup>3</sup>. The grain bulk modulus is  $K_s = 3.79 \times 10^{11}$  g/cm s<sup>2</sup>. In all examples the bore is of radius a = 10 cm and filled with drilling mud,  $\rho_B = 1.4$  g/cm<sup>3</sup>,  $v_B = 1250$  m/s. Intrinsic attenuation in the elastic frame has been ignored in these computations, although nominal Q values of 1000 were assumed. Only open pore interface conditions are considered.

As discussed in Appendix A, the inertial factor characterizing the pore-fluid drag is T=3. The critical frequency  $f_c=\varphi\eta/2\pi\kappa\rho_f\,T$  is given in Table 3. This frequency marks the transition of the diffusive Biot third wave to a propagating wave; at  $f=f_c$ , the Biot theory predicts peaks in the body-wave attenuations. The extent of this effect can be gauged from the Q for the shear wave. It follows from equations (A-10) and (A-11) that  $Q_s\sim 2\rho T/\phi\rho_f$  and ranges from a low of  $Q_s\approx 43$  for Teapot-water to a high of  $Q_s\approx 10^6$  for Fox Hill-gas.

#### Stoneley-wave phase speed

The effect of formation porosity on the Stoneley phase and group speeds has been amply discussed by Schmitt et al. (1988). Figure 4 is representative and shows the exact and

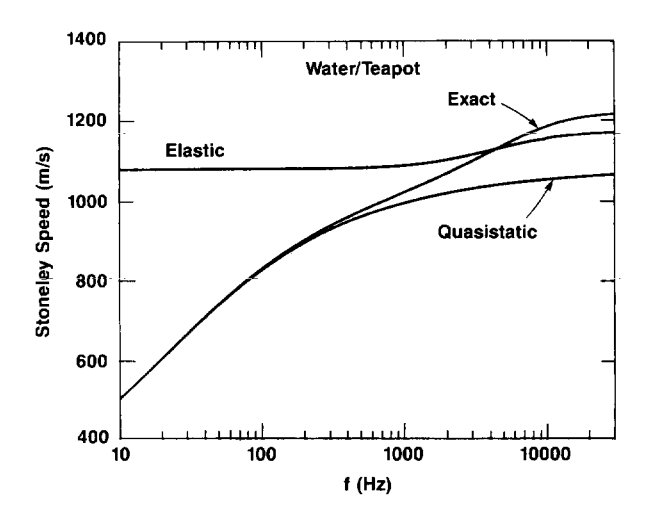


Fig. 4. The Stoneley phase speeds for water saturation of Teapot according to the poroelastic, elastic, and quasi-static theories.

336 Norris

quasi-static phase speed, equal to the real part of  $v = \omega/k$  computed from equations (23) and (13), respectively, for Teapot-water. This figure also shows the Stoneley phase speed for an equivalent elastic formation. The dispersion equation for a nonpermeable elastic formation (Biot, 1952) is given by the determinant of the  $3 \times 3$  submatrix formed from  $M_{ij}$ , i, j = 1, 2, 3 of equation (24) with  $B_C = B_S = 0$ . The compressional-wave and shear-wave numbers  $k_C$  and  $k_S$  are for an elastic solid of density  $\rho$ , shear modulus  $\mu$ , and bulk modulus  $K_c$ ; see Appendix A for precise definitions of these quantities.

Note the expected agreement between the quasi-static and dynamic theories as  $f \rightarrow 0$ . The transition from quasi-static to dynamic occurs at about 1 kHz. At higher frequencies, the phase speed exceeds the purely elastic speed. This is to be expected, since the pore fluid introduces attenuation and thus more dispersion. In typical, e.g., viscoelastic, wave processes exhibiting frequency-dependent attenuation, the effect upon the wave speed is to give a higher phase speed at higher frequencies. The same phenomenon is evident in Figure 4. Similar graphs for other combinations of formation and saturant show the same features as Figure 4. In particular the quasi-static theory faithfully reproduces the exact speeds for frequencies up to 1 kHz.

#### Stoneley-wave attenuation

Figure 5 compares the exact and quasi-static attenuations Im (k), calculated from equations (23) and (13), for oil saturation. Again, there is excellent agreement below 1 kHz. The exact attenuations ultimately exceed the quasi-static predictions, but can actually drop below the quasi-static values within a finite frequency range, particularly for Teapot which exhibits the greatest attenuation. Figure 6 illustrates the comparison for water saturation. Note the order-of-magnitude increase in attenuation as compared with values in Figure 5 for oil.

Consideration of the corresponding Stoneley-wave Q values, defined by  $v^{-1} = v_0^{-1}(1 + i/2Q)$ , where  $v_0$  is real, turns out to be more instructive. Figures 7 and 8 exhibit Q calculated by

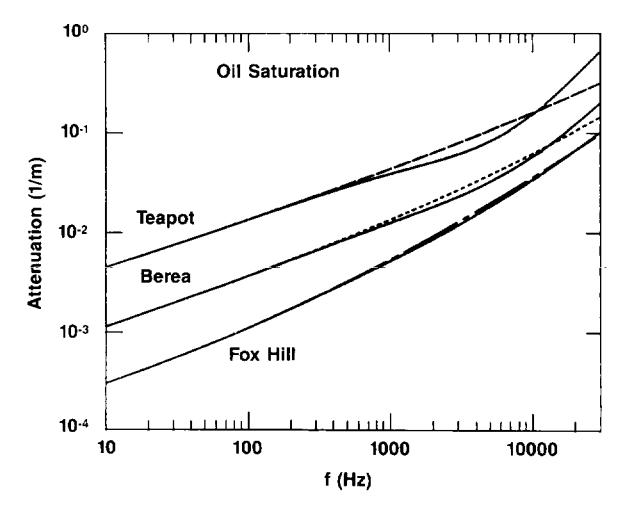


FIG. 5. Stoneley-wave attenuation for oil saturation. The solid line represents exact poroelastic theory. The other curves are the quasi-static theory.

the exact and quasi-static theories for oil and water saturation, respectively. With the exception of Teapot-water, which is discussed below, the curves of the exact dispersion relation suggest a peak in Q at high frequencies. This phenomenon, also apparent in Figure 5 of Schmitt et al. (1988), cannot be explained by the quasi-static approximation, but is apparently due to a high-frequency transition of the Stoneley wave in a curved bore to a Stoneley wave at a flat interface. This conclusion can be understood after a short analytical digression.

#### The Stoneley wave on a flat fluid-porous interface

The dispersion equation (23) contains in the limit  $a \to \infty$  the dispersion equation for interfacial waves at a flat fluid-porous interface. In this limit the terms in  $\mathbf{M}$  involving 1/a go to zero, and  $f_1(\xi_C a)$ ,  $f_1(\xi_B a)$ ,  $f_1(\xi_B a)$ , and  $f_2(\xi_B a)$  all tend to unity. The matrix  $\mathbf{M}$  further simplifies in the low-frequency regime  $\omega \ll \omega_c$  (see Appendix A). Thus,  $B_C$ ,  $B_S \sim 0$ ,  $B_D \sim B_0$ , and  $\xi_D \sim k_D \sim (i\omega/C)^{1/2}$ , where C is the diffusion coefficient of equation (7), and

$$\mathbf{M} \sim \begin{bmatrix}
\frac{-\xi_B \mu}{k_B^2 K_B} & k & \xi_C & (1+B_0)k_D \\
1 & 2k\xi_S & k_S^2 - 2k^2 & -2k^2 \\
0 & 2k^2 - k_S^2 & 2k\xi_C & 2kk_D \\
1 & 0 & \alpha \frac{M}{\mu} k_C^2 & (\alpha+B_0) \frac{M}{\mu} k_D^2
\end{bmatrix} (28)$$

Note that the low-frequency regime considered here is that in which the third wave in Biot's poroelastic theory is diffusive. It includes the quasi-static regime, but can go far beyond that regime. The latter is confined to 0–1 kHz, approximately. In the diffusive regime, the quantities  $k_{\gamma}/k_{D}$ ,  $\gamma=B$ , C, and S are small. Therefore, in evaluating det (M), certain terms in equation (28) can be set to zero. Specifically,  $M_{43} \rightarrow 0$  by subtracting  $[\alpha/(a+B_{0})](k_{C}^{2}/k_{D}^{2})$  times column 4 from column 3, and  $M_{24} \rightarrow 0$  by adding  $2k^{2}$  times column 1 to column 4. The

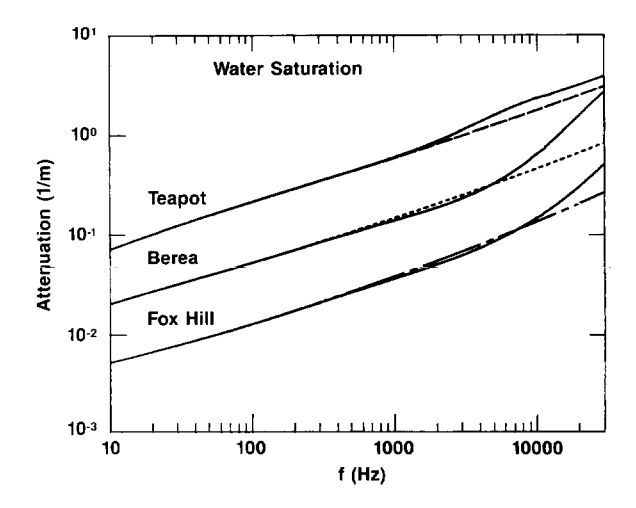


Fig. 6. The same as Figure 5 but for water infiltration.

dispersion relation then follows from equations (23) and (28) as

$$R + \frac{\rho_B}{\rho} \frac{\xi_C}{\xi_B} + \left(\frac{1}{\alpha + B_0}\right) \frac{K_B}{M} \frac{k_B^2}{\xi_B k_D} (B_0 R + 1 - 2k^2 k_S^{-2}) = 0, \quad (29)$$

where

$$R = 4k_S^{-4}k^2\xi_C\xi_S + (1 - 2k^2k_S^{-2})^2$$
 (30)

is the Rayleigh function for an elastic solid. Note that  $R + \rho_B \xi_C / \rho \xi_B = 0$  is the nondispersive equation for a fluid-elastic interface. In the latter case, the classic Stoneley wave is the only real root. The pore-flow effects are all contained in the final term in equation (29).

The pore-flow term in equation (29) can be simplified further by considering a very stiff frame, in which case it follows from Appendix A that  $|B_0| \gg 1$ ,  $M \sim K_f/\phi$ . Using these approximations, the dispersion relation becomes

$$R + \frac{\rho_B}{\rho} \frac{\xi_C}{\xi_B} + \phi R \frac{\rho_B}{\rho_f} \frac{k_B^2}{\xi_B k_D} = 0.$$
 (31)

The influence of the pore-flow term may be assessed by the low-frequency approximation valid in the diffusive regime,

$$\frac{k_B^2}{\xi_B k_D} \sim \frac{\sqrt{\omega C} \, e^{-i\pi/4}}{v_B \left[1 - (v_B/v)^2\right]^{1/2}},\tag{32}$$

where  $v = \omega/k$  is the complex Stoneley phase speed. Thus, the effect of pore flow *increases* with frequency for the flat interface.

**Explanation of Q maxima.**—The peaks in the data in Figures 7 and 8 can now be interpreted as a transition from curvature-dominated dispersion to that at an effectively flat interface. Beyond the peak, Q decreases according to equations (29) and (30). This hypothesis is vindicated by the data of Figures 9 and 10 showing Q for gas infiltration of Fox Hill and Berea. Note the extremely small Q values in these figures, illustrating the critically damped nature of the Stoneley wave for gas-saturated formations. This strongly evanescent character has been noted previously by Rosenbaum (1974) and Schmitt et al. (1988).

The presence of the *Q* maximum is to be expected for sandstone-saturant formations in which the flat interface approximation is justified. Thus, for water in Fox Hill and Berea and gas in Fox Hill, there exists a frequency range beyond the quasi-static regime for which the Biot third wave is diffusive and within which the above-mentioned transition is possible. This is only marginally true for Teapot-water and Berea-gas. A transition actually occurs in the latter case (Figure 10), but not in the former (Figure 8).

#### Discussion

The results indicate that the nature of Stoneley-wave dissipation in permeable formations is quite complex in the acoustic logging frequency range. The appearance of the Q maximum is essentially a transition from curvature-dominated dispersion to an effectively flat interface. The only pore-flow parameter contained in the approximate equation (32) is the diffusion coefficient C of equation (7). There are no inertial effects associated with the pore flow. This is just a reflection of

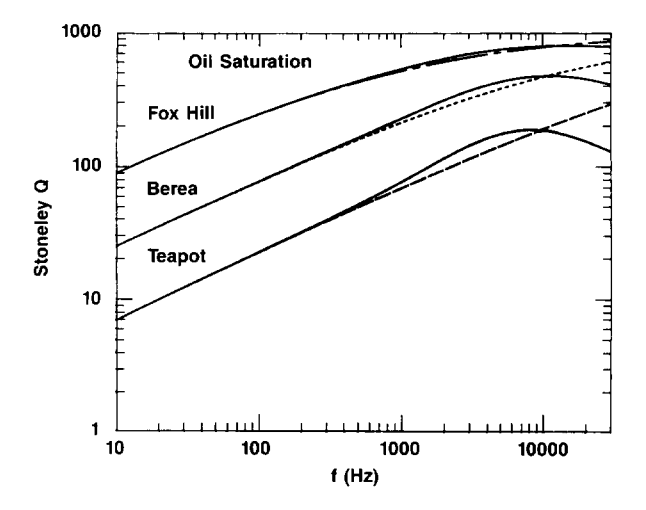


Fig. 7. The Q value of the Stoneley wave for oil saturation. The solid line represents exact poroelastic theory. The other curves are the quasi-static theory.

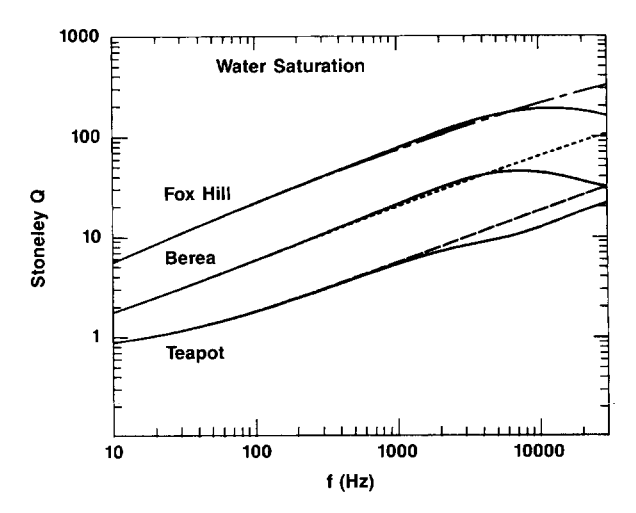


Fig. 8. The same as Figure 7 but with water as the pore saturant.

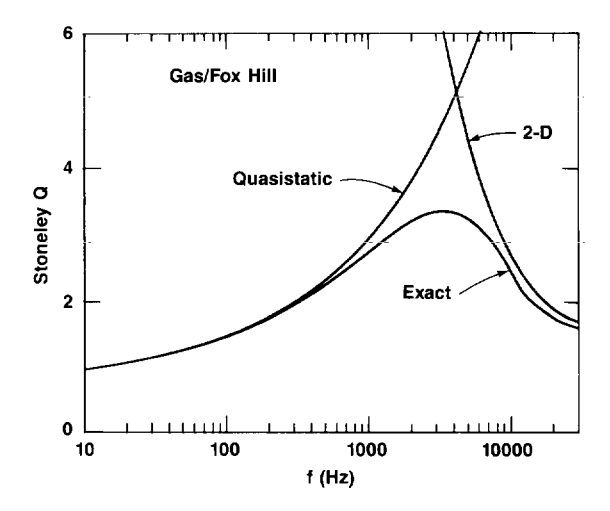


Fig. 9. The Stoneley Q value for gas-infiltrated Fox Hill. The 2-D curve is found by solving for the Stoneley wave at a flat interface from equations (29) and (30).

338 Norris

the fact that the approximation in equation (32) implicitly assumes the frequency is much less than the critical frequency  $f_c$  of the Biot theory [see equation (A-14)]. This is the frequency at which the inertial drag of the pore fluid becomes important and the pore-pressure propagation changes from diffusive to wave-like. Thus, the Q maximum is simply a result of Darcy viscous pore flow.

The results presented for the Stoneley-wave attenuation are in general agreement with the findings of Rosenbaum (1974). The transition from low-frequency to high-frequency behavior of the Stoneley Q is also noted by Schmitt et al. (1988), although they do not discuss its physical origin in detail. Many illustrative synthetic microseismograms are given by Schmitt and Bouchon (1984) and Schmitt et al. (1988) for Berea sandstone. Figures 11 and 12 display synthetic waveforms in Berea for different pulse center frequencies. The increasing Stoneleywave attenuation for oil, water, and gas saturation is evident in these figures. (Tangentially, it is interesting to note the pronounced effect of gas saturation on the shear waves. The shear-wave attenuation in the formation is too small to account for this. It must be due to decreased reflection and transmission at the interface.) The disappearance of the Stoneley wave is also graphically represented by the spectral density functions of Schmitt et al. (1988). However, in all these simulations, it is difficult to discern a Q maximum. In general, it is a difficult practical problem to measure the full frequency dependence of the Stoneley wave attenuation from synthetic data, let alone real data. For example, Stevens and Day (1986) estimate the error in the Stoneley Q to be about 10 percent for high quality, low noise waveform data in the range 1 to 4 kHz. Data of similar, or better, quality over a broader band are required if a peak in Q is to be observed.

#### CONCLUSIONS

Stoneley-wave attenuation and dispersion in permeable formations have been discussed for the full frequency range of acoustic logging. Separate analyses for the quasi-static and the fully dynamic behavior show that the former is adequate for sandstone formations up to at least 1 kHz. The quasi-static theory correctly accounts for frame compressibility. Comparison with White's (1983) quasi-static theory for a rigid frame shows that the effect of compressibility is to increase the tubewave attenuation, but only marginally for sandstone. Comparisons with other previous studies show that the tube-wave attenuation of Mathieu and Toksöz (1984) is erroneous at all frequencies, while the theory of Hsui and Toksöz (1986) is asymptotically correct in the quasi-static regime, but some of their numerical results are in error.

The fully dynamic dispersion relation for the Stoneley wave has been derived using Biot's (1962) theory of poroelasticity. Numerical computations of attenuation corroborate previous authors' findings on the effects of permeability, particularly those of Rosenbaum (1974) and Schmitt et al. (1988). The results show that the attenuation increases with permeability but depends critically on the pore saturant. The effects of oil saturation are minimal, while water can induce significant attenuation. However, the Stoneley wave can be critically damped for gas infiltration, suggesting that the presence of gas at or near the borehole interface could cause the Stoneley wave to disappear.

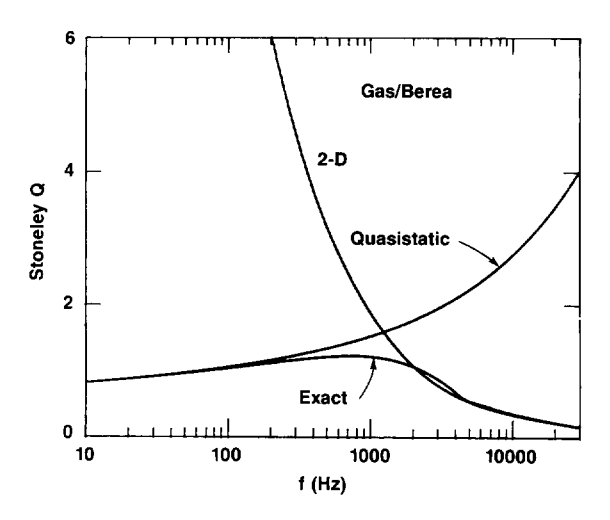


Fig. 10. The Q value for gas-saturated Berea.

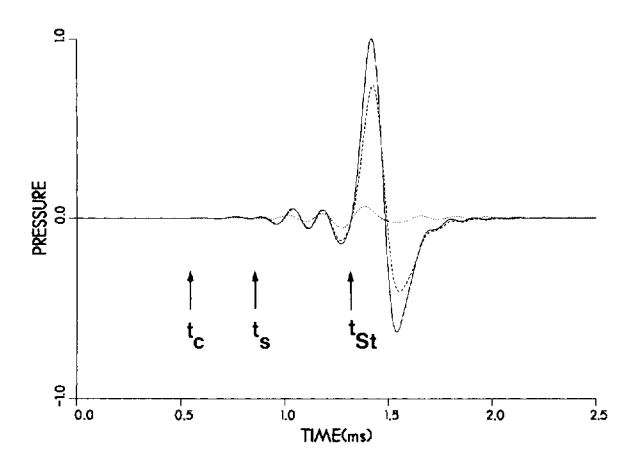


Fig. 11. The acoustic pressure on the axis of the borehole at a distance of 1.5 m from a point source of center frequency 2.5 kHz (see Appendix C). The bore fluid is drilling mud, the formation is saturated Berea with oil (solid curve), water (dashed curve), or gas (dotted curve).

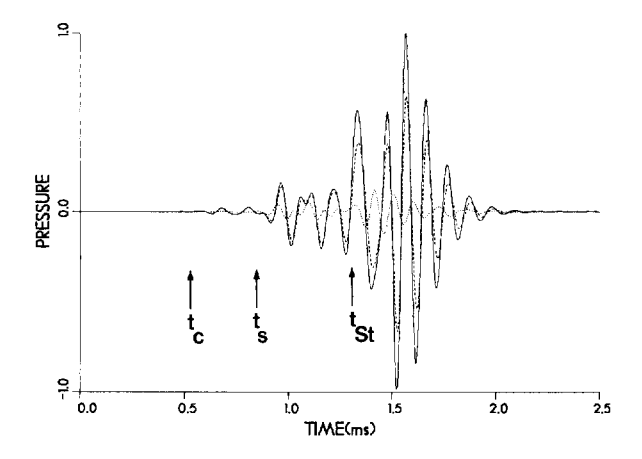


Fig. 12. The same as Figure 11, but for a pulse center frequency of 5 kHz.

The attenuation curves indicate that the O value of the Stoneley wave can display a peak in the acoustic logging band. This novel phenomenon has been explained on the basis of a transition from curvature-dominated dispersion to dispersion on a flat fluid-porous interface, an explanation which is supported by analytical approximation of the dispersion relation. The Q peak is not a quasi-static tube-wave effect, since the Q value increases as  $(f)^{1/2}$  in this regime. It is a combination of geometrical dispersion effects and the dissipation caused by viscous flow in the pores. It is not a product of pore-fluid inertial effects contained in the Biot theory, but is simply a direct consequence of Darcy's law. High-quality real data are necessary to determine whether the Q peak is of practical significance. Variations in bed properties and intrinsic attenuation may dominate, making a peak difficult to identify. However, observation of a peak would considerably enhance confidence in models such as Biot theory.

#### **ACKNOWLEDGMENTS**

My thanks to L. Guan for numerical assistance, and to the referee for a thorough review and for providing extensive references. This work was supported by Exxon Research and Engineering Company, and also by the National Science Foundation (Grant no. MDM-85-16256). Acknowledgment is made to the donors of the Petroleum Research Fund, administered by the American Chemical Society, for partial support of this research. Dedicated to the memory of N. J. Norris.

#### REFERENCES

- Alhilali, K. A., and Zemanek, J., 1984, Determination of formation permeability from a long-spaced acoustic log: U.S. patent no. 4 432 077.
- Berryman, J. G., and Thigpen, L., 1985, Linear dynamic poroelasticity with micro-structure for partially saturated porous solids: J. Appl. Mech., **52**, 345–350.
- Biot, M. A., 1952, Propagation of elastic waves in a cylindrical bore containing a fluid: J. Appl. Phys., 23, 997-1005.
- 1956, Theory of propagation of elastic waves in a fluidsaturated porous solid, I. Low frequency range: J. Acoust. Soc. Am., 28, 168-178.
- 1962, Mechanics of deformation and acoustic propagation in porous media: J. Appl. Phys., 33, 1482-1498.
- Brown, R. J. S., 1980, Connection between formation factor for electrical resistivity and fluid-solid coupling factor in Biot's equations for acoustic waves in fluid-filled porous media: Geophysics, 45, 1269-1275
- Brown, R. J. S., and Korringa, J., 1975, On the dependence of the elastic properties of a porous rock on the compressibility of the pore fluid: Geophysics, 40, 608-616.
- Burns, D. R., and Cheng, C. H., 1986, Determination of in situ per-

- meability from tube wave velocity and attenuation: Trans., Soc. Prof. Well-log Anal. 27th Ann. Logg. Symp., paper KK.
  Burridge, R., and Keller, J. B., 1981, Poroelasticity equations derived
- from microstructure: J. Acoust. Soc. Am., 70, 1140-1146. Chandler, R., and Johnson, D. L., 1981, The equivalence of quasistatic flow in fluid saturated porous media and Biot's slow wave in the limit of zero frequency: J. Appl. Phys., 52, 3391-3395.
- Deresiewicz, H., and Skalak, R., 1963, On uniqueness in dynamic poroelasticity: Bull., Seis. Soc. Am., 53, 783-788.

  Hashin, Z., 1962, The elastic moduli of heterogeneous materials: J.
- Appl. Mech., 29, 143-150.
- Hsui, A. T., and Toksöz, M. N., 1986, Application of an acoustic model to determine in situ permeability of a borehole: J. Acoust.
- Soc. Am., 79, 2055–2059.

  Jaeger, J. C., and Cook, N. G. W., 1969, Fundamentals of rock mechanics: Methuen.
- Johnson, D. L., Plona, T. J., and Scala, C., 1982, Tortuosity and acoustic slow waves: Phys. Rev. Lett., 49, 1840-1844.
- Johnson, D. L., Plona, T. J. and Kojima, H., 1987, Probing porous media with 1st sound, 2nd sound, 4th sound and 3rd sound, in Banavar, J. R., Koplik, J., and Winkler, K. N., Eds., Physics and chemistry of porous media, II: Am. Inst. Phys., Conf. Proc. 154, 243 - 277
- Johnson, D. L., Koplik, J., and Dashen, R., 1987, Theory of dynamic permeability and tortuosity in fluid saturated porous media: J. Fluid Mech., 176, 379-402.
- Kurkiian, A. L., 1985, Numerical computation of individual far-field arrivals, excited by an acoustic source in a borehole: Geophysics, **50**, 852–866
- Liu, H. L., 1988, Borehole modes in a cylindrical fluid-saturated permeable medium: J. Acoust. Soc. Am., 84, 424-431.
- Marsily, G. de, 1981, Hydrogeologie quantitative: Masson.
- Mathieu, F., 1984, Application of full waveform acoustic logging data to the estimation of reservoir permeability: M.Sc. thesis, MIT.
- Mathieu, F., and Toksöz, M. N., 1984, Application of full waveform acoustic logging data to the estimation of reservoir permeability: 54th Ann. Internat. Mtg., Soc. Expl. Geophys., Expanded Abstracts, 9-12.
- Norris, A. N., 1986, On the viscodynamic operator in Biot's equations of poroelasticity; J. Wave-Material Interaction, 1, 365-380.
- Pascal, H., 1986, Pressure wave propagation in a fluid flowing through a porous medium and problems related to interpretation of Stoneley's wave attenuation in acoustic well logging: Int. J. Eng. Sci., 24, 1553-1570.
- Rice, J. R., and Cleary, M. P., 1976, Some basic stress diffusion solutions for fluid saturated elastic porous media with compressible constituents: Rev. Geophys. Space Phys., 14, 227-241.
- Rosenbaum, J. H., 1974, Synthetic microseismiograms—logging in a porous formation: Geophysics, 39, 14-32.
- Schmitt, D. P., and Bouchon, M., 1984, Full wave synthetic acoustic logs in saturated porous media: 54th Ann. Internat. Mtg., Soc. Expl. Geophys., Expanded Abstracts, 17-20.
  - 1985, Full-wave acoustic logging: synthetic microseismograms and frequency-wavenumber analysis: Geophysics, 50, 1756–1778.
- Schmitt, D. P., Bouchon, M., and Bonnet, G., 1988, Full-wave synthetic acoustic logs in radially semiinfinite saturated porous media: Geophysics, 53, 807-823.
- Stevens, J. L., and Day, S. M., 1986, Shear velocity logging in slow formations using the Stoneley wave: Geophysics, 51, 137-147.
- White, J. E., 1983, Underground sound: Elsevier Science Publ. Co.
- Williams, D. M., Zemanek, J., Angona, F. A., Dennis, C. L., and Caldwell, R. L., 1984, The long space acoustic logging tool: Trans., Soc. Prof. Well-log Anal. 25th Ann. Logg. Symp., p. 16.

#### APPENDIX A

#### Biot's equations of dynamic poroelasticity

Following the notation of Biot (1962), the bulk stress tensor is  $\tau_{ij}$  and the pore-fluid pressure is p. The relative fluid displacement is  $\mathbf{w} = \phi(\mathbf{U} - \mathbf{u})$ , where  $\mathbf{u}$  and  $\mathbf{U}$  are the solid matrix and pore-fluid displacements, respectively. The isotropic stress-strain relations are

$$\tau_{ij} = K_c e_{kk} \delta_{ij} + 2\mu (e_{ij} - \frac{1}{3} e_{kk} \delta_{ij}) + \alpha M w_{k,k} \delta_{ij}, \quad (A-1)$$

and

$$p = -Mw_{k,k} - \alpha Me_{kk}, \tag{A-2}$$

where  $e_{ij} = 1/2(u_{i,j} + u_{j,i})$ ,  $u_{i,j} = \partial u_i/\partial x_j$ , and the summation convention is assumed. The bulk modulus  $K_c$  is that of the undrained medium  $(w_{k,k} = 0)$ . The corresponding drained (p = 0) bulk modulus is K, related to  $K_c$  by the Biot-Gassmann relation:

$$K_c = K + \alpha^2 M. \tag{A-3}$$

The quantity  $\alpha$  is

$$\alpha = 1 - \frac{K}{K_s},\tag{A-4}$$

where  $K_s$  may be identified as the bulk modulus of the solid

340 Norris

grain (Brown and Korringa, 1975; Rice and Cleary, 1976). The modulus M is

$$M = \left[ \frac{\Phi}{K_f} + \frac{(\alpha - \phi)}{K_s} \right]^{-1}, \tag{A-5}$$

where  $K_f$  is the fluid bulk modulus, and  $\phi$  the porosity. The shear modulus  $\mu$  in equation (A-1) is the same under drained and undrained conditions. The above equations simplify to equation (2) for a rigid matrix, which follows from equations (A-2) and (A-5) with  $\alpha \to 0$  and  $K_s \to \infty$ .

The bulk equations of motion are

$$\tau_{ij,j} = \rho \frac{\partial^2 u_i}{\partial t^2} + \rho_f \frac{\partial^2 w_i}{\partial t^2}.$$
 (A-6)

where  $\rho_f$  is the fluid density,  $\rho = \phi \rho_f + (1 - \phi)\rho_s$ , and  $\rho_s$  is the solid or grain density. The pore-fluid equations of motion are

$$-p_{ji} = \rho_f \frac{\partial^2 u_i}{\partial t^2} + \angle w_i, \qquad (A-7)$$

where / is a linear viscodynamic operator (Norris, 1986; Johnson, Koplik, and Dashen, 1987). In its simplest form (Biot, 1956),

$$\angle w_i = m \frac{\partial^2 w_i}{\partial t^2} + \frac{\eta}{\kappa} \frac{\partial w_i}{\partial t}, \tag{A-8}$$

where  $m = T \rho_f/\phi$ , and T is an inertial factor satisfying T > 1. This factor is discussed by Brown (1980), Norris (1986), and Johnson, Koplik, and Dashen, (1987), among others. Equation (A-8) is discussed below.

**Plane-wave solutions.**—There are three plane-wave solutions to equations (A-6) and (A-7),

$$(\mathbf{u}, \mathbf{w}) = (\mathbf{a}, B_{\mathbf{v}} \mathbf{a}) \exp \left[i(k_{\mathbf{v}} \mathbf{b} \cdot \mathbf{x} - \omega t)\right],$$
 (A-9)

where **b** is any real unit vector, and  $\gamma = C$ , S, and D, for compressional wave, shear wave, and diffusive wave, respectively. The polarization vector **a** is parallel to **b** for C and D, and perpendicular for S. The complex wavenumbers  $k_{\gamma}$ , phase speeds  $v_{\gamma} = \omega/v_{\gamma}$ , and fluid-motion amplitudes  $B_{\gamma}$  are all frequency-dependent. Thus,

$$v_S = v_{S0} \left( 1 + \frac{\rho_f}{\rho} B_S \right)^{-1/2},$$
 (A-10)

$$B_{\rm S} = \frac{-\rho_f}{m} \left( 1 + \frac{i\omega_c}{\omega} \right)^{-1},\tag{A-11}$$

and for  $\gamma = C$  and D,

$$v_{\gamma} = v_{C0} \left( \frac{1 - B_{\gamma}/B_0}{1 + B_{\gamma}\rho_f/\rho} \right)^{1/2},$$
 (A-12)

$$\frac{B_c}{B_b} = \frac{1}{2} B_0 \left\{ \delta \mp \left[ \delta^2 - 4\alpha (1 - \delta) / B_0 \right]^{1/2} \right\}.$$
 (A-13)

Here,  $v_{S0} = (\mu/\rho)^{1/2}$  and  $v_{C0} = [(K_c + 4\mu/3)/\rho]^{1/2}$  are the zero-frequency limits of  $v_C$  and  $v_S$ . Also,

$$\omega_{c} = \frac{1}{m} \frac{\eta}{\kappa}, \tag{A-14}$$

$$B_0 = -\left(\frac{K_c + \frac{4}{3}\mu}{\alpha M}\right),\tag{A-15}$$

and

$$\delta = \frac{\alpha - \frac{\rho B_S}{\rho_f B_0}}{\alpha + B_S}.$$
 (A-16)

The critical frequency  $\omega_c$  marks the transition of the viscodynamic operator from the low-frequency, Darcy regime dominated by viscous flow ( $\omega < \omega_c$ ) to the high-frequency regime ( $\omega > \omega_{\perp}$ ) in which the inertial drag of the pore fluid is dominant. Note that for  $\omega \ll \omega_c$ ,  $v_C \sim v_{CO}$ ,  $v_S \sim v_{SO}$ , and  $B_C$ ,  $B_S \sim 0$ . Also in the low-frequency regime,  $B_D \sim B_0 < 0$ , and  $k_D \sim (i\omega/C)^{1/2}$ , where C is the diffusion coefficient of equation (7). Note that  $\delta = 1$ , or  $B_0 + \rho/\rho_f = 0$ , is the dynamic compatibility condition of Biot (1956). The negative constant  $B_0$ , which determines the relative magnitude of the fluid and matrix motions for the diffusion process, depends upon the elastic moduli but not on the inertial terms. It is always less than -1 for fluids that are more compressible than the matrix grain, and  $B_0 \approx -1$  for nearly unconsolidated media like soil. For fluids that are much more compressible than the matrix, as in most sandstones,  $B_0 \approx -(\phi/\alpha)(K_c + 4\mu/3)/K_f$ , so  $B_0$  is large and negative.

#### The viscodynamic operator

The viscodynamic operator  $\angle$  in equation (A-8) includes the static Darcy's law term plus an inertial correction. It can be shown (Norris, 1986) that both  $\kappa$  and m depend upon the solution of a single Stokes flow problem through the porous network. The permeability k comes from the average flow rate in the direction of applied pressure gradient, which is the usual definition of permeability. The inertia m, or alternatively the factor T > 1, depends upon the mean square velocity in the pores under the same pressure gradient. Thus, both  $\kappa$  and Tcan be viewed as independent measurable quantities. Measurement of  $\kappa$  is straightforward. Despite the discussion of experimental data in Pascal (1986), it appears that there are no relevant measurements of T available. However, it can be estimated from electrical formation factor data as follows. One can extend the definition of T to higher frequencies, and prove that  $T(0) \ge T(\omega)$  (Brown, 1980), where T(0) is the value in equation (A-8). The electrical formation factor is equal to  $T(\infty)/\phi$  (Brown, 1980; Johnson et al., 1982). Measured values of  $T(\infty)$  ranging from 1.8 to 3.8 have been reported for sandstone-like materials (Johnson et al., 1982; Johnson, Plona, and Kojima, 1987). Brown's inequality makes these values lower bounds for the T in equation (A-8). Based upon these considerations, the value T = 3 has been used in all the numerical calculations reported here.

Alternatively, the operator  $\angle$  can be defined by an effective permeability through the factor  $F(\omega)$ ,

$$\angle w_i = \frac{-i\omega\eta}{\kappa} F(\omega) w_i. \tag{A-17}$$

Thus,  $F(\omega) = 1 - i\omega/\omega_c$  for equation (A-8). Biot (1956) proposed extending  $F(\omega)$  to higher frequencies by modeling the pore network as circular tubes. His prescription is not consistent with a rigorous definition of the viscodynamic operator (Norris, 1986 and references therein), but when corrected

becomes

$$F(\omega) = \frac{i3\omega}{4\omega_c} \frac{J_0(\sqrt{6i\omega/\omega_c})}{J_2(\sqrt{6i\omega/\omega_c})}.$$
 (A-18)

For  $\omega \ll \omega_c$ ,  $F(\omega) \sim 1 - i\omega/\omega_c$ . Other authors have used  $F(\omega)$  in a form similar to equation (A-18). This strategy is not adopted here. Rather,  $\kappa$  and m in equation (A-8) are considered empirical constants to be determined, and no explicit pore geometry is considered.

#### Borehole dispersion equation

Let  $\mathbf{u}^B$  and  $p^B$  be the displacement and pressure fields in the borehole fluid, r < a in cylindrical coordinates. The four boundary conditions at the interface are continuity of average normal displacement, continuity of normal stress, continuity of shear stress, and continuity of fluid pressure (open pores):

$$u_r^B(a) = u_r(a) + w_r(a),$$
 (A-19)

$$-p^{B}(a) = \tau_{r}(a), \tag{A-20}$$

$$0 = \tau_{ra}(a), \tag{A-21}$$

and

$$p^{B}(a) = p(a). \tag{A-22}$$

The solution method assumes a potential function for each of the four bulk waves. For r < a,

$$\mathbf{u}^B = A_B \nabla J_A (\xi_B r) e^{i(kz - \omega t)}, \tag{A-23}$$

and for r > a,

$$\mathbf{u} = \left[ A_C \nabla H_0^{(1)}(\xi_C r) + A_D \nabla H_0^{(1)}(\xi_D r) + A_S \left( \mathbf{e}_z \frac{1}{r} \frac{\partial}{\partial r} r - \mathbf{e}_r \frac{\partial}{\partial z} \right) H_1^{(1)}(\xi_S r) \right] e^{i(kz - \omega r)}, \quad (A-24)$$

$$\mathbf{w} = \begin{bmatrix} A_C B_C \nabla H_0^{(1)}(\xi_C r) + A_D B_D \nabla H_0^{(1)}(\xi_D r) \\ & - A_D B_D \nabla H_0^{(1)}(\xi_D r) \end{bmatrix}$$

$$+ A_S B_S \left( \mathbf{e}_z \frac{1}{r} \frac{\partial}{\partial r} r - \mathbf{e}_r \frac{\partial}{\partial z} \right) H_1^{(1)}(\xi_S r) \left[ e^{i(kz - \omega t)}, \quad (A-25) \right]$$

where

$$\xi_{y} = (k_{y}^{2} - k^{2})^{1/2}$$
, Im  $(\xi_{y}) \ge 0$ ,  $\gamma = B$ , C, S, D, (A-26)

and  $k_B = \omega/v_B$ . The frequency-dependent complex numbers  $B_C$ ,  $B_S$ , and  $B_D$  are defined above. Substituting equations (A-24) and (A-25) into the boundary conditions (A-19)–(A-22) gives the set of equations  $\mathbf{M}[A_B, A_S, A_C, A_D]^T = \mathbf{0}$ , where  $\mathbf{M}$  is defined in equation (24). The necessary condition for a solution is equation (23).

#### APPENDIX B

#### The inequality $\alpha > \phi$

The maximum possible value of K gives the minimum possible value of  $\alpha$  in equation (A-4). The Hashin-Shtrikman bounds (Hashin, 1962) for a two-phase composite give an upper bound on K. In this case, one phase is the solid grain, with elastic moduli  $K_s$  and  $\mu_s$ , and the other phase is vacuum. Then  $K \leq K_G$ , where

$$K_G = \frac{(1 - \phi)K_s}{1 + \phi 3K_s/4\mu_s}.$$
 (B-1)

The lower bound on  $\alpha$  follows from equations (B-1) and (A-4) as

$$\alpha \ge \phi + \frac{\phi(1-\phi)}{\phi + 4\mu_s/3K_s}.$$
 (B-2)

Thus,  $\alpha > \phi$ .

#### APPENDIX C

#### Solution for a point source in the borehole

Let  $p^{B(0)}$  be the time harmonic point-source pressure in an infinite bore fluid,

$$p^{B(0)} = \frac{e^{i(K_B R - \omega t)}}{4\pi R}$$

$$= \int_0^\infty A_0 H_0^{(1)}(\xi_B r) e^{i(kz - \omega t)} dk, \qquad (C-1)$$

where  $R = \sqrt{r^2 + z^2}$ ,  $A_0 = i/8\pi$ , and  $\xi_B$  follows from equation (A-26). In the presence of the formation, the pressure becomes

$$p^{B} = \int_{-\infty}^{\infty} dk \ e^{i(kz - \omega t)} \left\{ A_{0} H_{0}^{(1)}(\xi_{B} r) + A_{B} J_{0}(\xi_{B} r) \right\}, \quad (C-2)$$

where  $A_B$  follows from satisfaction of equations (A-19)–(A-22)

$$A_{B}(\omega, k) = -A_{0} \frac{H_{0}^{(1)}(\xi_{B} a)}{J_{0}(\xi_{B} a)} \frac{\bar{D}(\omega, k)}{D(\omega, k)},$$
 (C-3)

and  $\bar{D}(\omega, k)$  is the same as  $D(\omega, k)$  of equation (23), but with  $f_2(\xi_B a)$  in  $M_{11}$  of equation (24) replaced by  $-1/f_1(\xi_B a)$ .

Synthetic waveforms were computed using an adaptive integration scheme for equation (C-2), combined with an FFT. The source spectrum used was the second derivative of a Blackman-Harris window, from Kurkjian (1985). There is a typographical error in Kurkjian's constant  $b_1$ ; it should read  $b_1 = -0.48829$ .